Effect of Magnetic Ordering on the Stability of Ni–Mn–Ga(–Co–Cu) Alloys Along the Tetragonal Deformation Path

Zelený, Martin; Sozinov, Alexei; Björkman, Torbjörn; Straka, Ladislav; Heczko, Oleg; Nieminen, Risto M.

Published in:
IEEE Transactions on Magnetics

DOI:
10.1109/TMAG.2017.2707527

Published: 01/01/2017

Document Version
Accepted author manuscript

Document License
Unknown

Effect of Magnetic Ordering on the Stability of Ni-Mn-Ga(-Co-Cu) Alloys along the Tetragonal Deformation Path

Martin Zelený[1,2], Alexei Sozinov[3], Torbjörn Björkman[4], Ladislav Straka[2,5], Oleg Heczko[2,5] and Risto M. Nieminen[6]

[1]Institute of Materials Science and Engineering, NETME Centre, Faculty of Mechanical Engineering, Brno University of Technology, Brno, CZ-61669, Czech Republic
[2]Faculty of Mathematics and Physics, Charles University, Prague, CZ-12116, Czech Republic
[3]Material Physics Laboratory, Lappeenranta University of Technology, Savonlinna, FI-57170, Finland
[4]Physics/Department of Natural Sciences, Åbo Akademi University, Turku, FI-20500, Finland
[5]Institute of Physics, Academy of Sciences of the Czech Republic, Prague, CZ-18221, Czech Republic
[6]COMP/Department of Applied Physics, Aalto University School of Science, Aalto, FI-00076, Finland

The influence of magnetic ordering on the stability of Ni-Mn-Ga(-Co-Cu) Heusler alloys is investigated using the first-principles exact muffin-tin orbital method in combination with the coherent-potential approximation. The paramagnetic state is described by disordered local moment approach. In stoichiometric Ni_2MnGa alloy, the total energy profile along the tetragonal deformation path differs between ferromagnetic ground state and paramagnetic state with high energy, where cubic structure of austenite exhibits lower total energy than tetragonally distorted structure of martensite. Martensitic structure is stabilized in ground state by ferromagnetic interaction. In paramagnetic state it can be stabilized by partial substitution of Ni by Co or by partial substitution of Mn/Ga by Cu. Energy difference between paramagnetic and ferromagnetic state $\Delta E_{\mathrm{PM\text{-}FM}}$ can be used for qualitative estimation of Curie temperature T_C. Since Co doping to Ni sublattice slightly increases $\Delta E_{\mathrm{PM\text{-}FM}}$, the T_C should also increase, which corresponds to experimental findings. Analogically, Cu doping to Mn sublattice strongly decrease $\Delta E_{\mathrm{PM\text{-}FM}}$, which corresponds to strong decreasing of T_C also confirmed experimentally. For Cu doping in Ga sublattice the decrease in T_C is weaker.

***Index Terms*— Ab initio calculation, Curie temperature, Ni-Mn-Ga, magnetic shape memory alloys.**

I. Introduction

THE functional properties of magnetic shape memory Heusler alloys originate from the coupling between the ferromagnetic microstructure and ferroelastic martensitic microstructure. The Ni-Mn-Ga system is unique in that it additionally exhibits extraordinarily high mobility of martensitic twin boundaries. That results in interesting magnetomechanical effects such as a giant magnetic-field-induced strain (MFIS), known also as the magnetic shape memory (MSM) effect or magnetically induced reorientation (MIR) [1], [2]. The control of material properties related to structural and magnetic phase transitions, especially martensitic transformation temperature T_M and Curie temperature T_C, is important for potential engineering applications in actuators, sensors, vibrational energy harvesters [3], or magnetic refrigeration systems [4].

For stoichiometric Ni_2MnGa, the transformation from austenite with cubic $L2_1$ structure to tetragonal martensite with five-layered modulation (10M) occurs at T_M = 202 K, whereas T_C is about 376 K [5]. The 10M martensite exhibits up to 6% MFIS [6], [7]. Recent electronic structure calculations predict orthorhombic structure with four-layered modulation (4O) as a ground state at 0 K [8] for Ni_2MnGa alloy but so far there is no experimental report.

The exact composition of alloy has a strong influence on the structure of martensitic phase and transformation temperature T_M. For example alloys with excess concentration of Mn on the account of Ga exhibit increased T_M and orthorhombic lattice with seven-layered modulation (14M martensite) and nearly 10% MFIS [9]. Both 10M and 14M martensite exhibit $c/a < 1$. The third martensitic phase exhibits nonmodulated (NM) tetragonally distorted $L2_1$ structure with $(c/a)_{\mathrm{NM}} \approx 1.17–1.23$ and is typical for larger deviation from stoichiometry where T_M reaches to 400 K [10].

The effect of chemical composition on T_C is much weaker than on T_M. The Curie temperature decreases only slightly with increasing concentration of Ni instead of Mn until it decreases below T_M at certain composition [11], [12]. Similar behavior of T_C has also been observed in the alloys with the substitution of Mn for Ga [10], [13]. The Curie temperatures may differ for austenite and martensite phase, i.e. $T_C^A \neq T_C^M$. The effect of composition on each phase is different, because T_C^M decreases much faster than T_C^A with increasing concentration of Mn [10]. The influence of the tetragonality of martensite on the exchange interactions in Ni_2MnGa alloy and subsequently on T_C have been discussed by Galanakis and Şaşıoğlu [14].

The alternative way to manipulate the transformation temperatures is by adding new elements into the alloy. Replacing a small fraction of Ni by Co will increase T_C^A but will decrease T_M [15]. Recent classical Monte Carlo

Manuscript received April 1, 2015; revised May 15, 2015 and June 1, 2015; accepted July 1, 2015. Date of publication July 10, 2015; date of current version July 31, 2015. (Dates will be inserted by IEEE; "published" is the date the accepted preprint is posted on IEEE Xplore®; "current version" is the date the typeset version is posted on Xplore®). Corresponding author: M. Zelený (e-mail: zeleny@fme.vutbr.cz).

Color versions of one or more of the figures in this paper are available online at http://ieeexplore.ieee.org.

Digital Object Identifier (inserted by IEEE).

simulations in combination with first-principle approach reveal that T_C^M will also decrease with increasing Co concentration [16]. Replacing part of Mn/Ga by Cu increases T_M and decreases T_C [17], [18]. Such changes in transformation temperatures results from the competition between the covalent-like hybridization of Ga-Ni and Ga-Mn interactions and the magnetic interaction of Mn atoms which is influenced by the presence of dopants [16], [19]-[21]. The simultaneous Co- and Cu-doping has been successfully used for tuning of transformation temperatures: The alloy with composition $Ni_{46}Co_4Mn_{24}Ga_{22}Cu_4$ exhibits transformation temperatures T_M = 330 K and T_C^A = 393 K. Moreover, due to the dopants, this alloy exhibits reduced lattice tetragonality and 12% MFIS in NM phase, which is the largest MFIS reported so far [22], [23].

Ab initio (or first-principles) calculations of electronic structure based on density functional theory [24], [25] have been employed to explain doping effects in Ni-Mn-Ga system. Li *et al.* used exact muffin-tin-orbital (EMTO) method in combination with coherent potential approximation (CPA) for investigation of site preference and elastic constants. [26]. Co exhibits a strong tendency to occupy the Ni sublattice in all types of composition and Cu atoms always occupy the sublattice of the host elements in deficiency.

The energy difference between the austenite and the nonmodulated martensite phase $\Delta E_{\text{A-NM}}$ obtained from *ab initio* calculations corresponds to experimentally determined T_M; larger difference in total energies indicates a higher T_M [27]. Our previous works [28], [29] analyzed the development of calculated total energies along the tetragonal deformation path for Co- and Cu-doped alloys to find $\Delta E_{\text{A-NM}}$ and explain changes in T_M. The analysis shows that doping effects can be well estimated using a linear superposition of the effects of individual dopants for alloys doped simultaneously by Co in Ni site and Cu in Ga or Mn site (general formula $Ni_{50-x}Co_xMn_{25-y}Ga_{25-z}Cu_{y+z}$).

Estimating T_C from *ab initio* calculations [16], [30]-[32] is a demanding task involving knowledge of pair exchange interaction parameters [33]. A qualitative prediction of changes in T_C can be done by calculation of energy difference between energies of ferromagnetic (FM) and paramagnetic (PM) state [34], [35]. The PM state can be well approximated by the disorder local moment (DLM) formalism within the CPA description. In this model the random orientation of local magnetic moments is described by random distribution of oppositely oriented local magnetic moments with equal concentrations [36].

The purpose of this paper is to reveal how the Co and Cu doping and magnetic interaction influences on the phase stability in austenite as well as in martensite with the NM structure. We present a detailed and comprehensive first-principles investigation of total-energy behavior along the tetragonal deformation path for different magnetic states to find equilibrium NM structure and estimate the energy differences $\Delta E_{\text{PM-FM}}$ between PM and FM states for different alloy compositions. This parameter is important for understanding of doping influence on T_C.

II. Computational Methods

The first principle calculations were carried out using exact muffin-tin-orbital (EMTO) method [37]-[39]. In combination with the full charge density (FCD) technique for total energy calculations [40], the EMTO method can accurately describe the total energy with respect to anisotropic lattice distortions such as tetragonal deformation. The chemical disorder caused by doping as well as magnetic disorder were included by using of the coherent-potential approximation (CPA) [41], [42]. This approximation does not take into account short-range interactions and atomic relaxations around the doping atoms, however, in full Heusler alloys, such short-range effects only have a negligible influence on the total energy landscape [43]. Contribution of these effects to the total energy is not bigger than 0.05 mRy/atom in case of Ni_2MnGa as was shown in our previous study [44]. The exchange correlation was described using the Perdew-Burke-Ernzerhof (PBE) generalized gradient approximation [45], employing the scalar-relativistic and soft-core approximations. The *s*, *p*, *d*, and *f* orbitals were included in the EMTO basis sets. The Ni $3d^8 4s^2$, Mn $3d^5 4s^2$, Ga $3d^{10} 4s^2 4p^1$, Co $3d^7 4s^2$, and Cu $3d^{10} 4s^1$ were treated as valence states. The Green's function was calculated for 32 complex energy points distributed exponentially on a semicircular contour. In order to obtain the best agreement with experiments for a $(c/a)_{\text{NM}}$, we introduced an additional optimization of the muffin-tin potential on the Ni sublattice as in [46] and [47] by choosing the atomic radius $R_{ws}^{\text{Ni}} = 1.10R_{ws}$ and overlapping potential spheres $R_{mt}^{\text{Ni}} = 0.95R_{ws}$, where R_{ws} is the average Wigner-Seitz radius. For the other sublattices, the usual setup $R_{mt} = R_{ws}$ was used. The effect of the charge misfit on the spherical potential is taken into account using the screened impurity model (SIM) by Korzhavyi *et al.* [48], [49]. In the one-center expansion of the full charge density, the number of components was truncated at 8. The Brillouin zone was sampled by a 13 × 13 × 13 uniform *k*-point mesh without any smearing technique.

The spin polarized version of the density functional theory [24], [25] was employed to treat the FM state. The spin disordered magnetic structure of PM state was simulated using the disordered local moment (DLM) formalism within the CPA, where the magnetic disorder was represented by randomly distributed Mn, and Ni(Co) atoms with up spin or down spin [36]. Beside the magnetic states this study includes also nonmagnetic (NonM) state of stoichiometric Ni_2MnGa calculated without spin polarization.

Four types of doping were considered based on previous theoretical studies and experiments: 2.5 % and 5% of Co in Ni sublattice and 5% of Cu in Mn or Ga sublattice. For each composition we calculated at a corresponding constant volume a series of total energies as a function of c/a in the range between c/a = 0.9 and 1.4, which describes the tetragonal deformation of austenite phase with $L2_1$ structure (c/a = 1). Differences between equilibrium volumes of austenite and NM martensite were neglected, because they have just a small effect on calculated total energies. Their average was used instead [28]. All calculated total energies along the deformation path were related to the energy of cubic structure

for alloy with given composition.

III. RESULTS

At first we compared the behavior of stoichiometric Ni_2MnGa in ferromagnetic (FM), paramagnetic (PM) and non-magnetic (NonM) state in order to reveal the effect of magnetic ordering on the stability of the phases.

FIG. 1 HERE

The total energy along the tetragonal deformation path in FM state is displayed in Fig. 1. It exhibits a local minimum at c/a = 1 which corresponds to austenite, whereas the global minimum at $(c/a)_{NM}$ = 1.256 corresponds to NM marteniste. Energy difference between the two phases, $\Delta E_{A\text{-}NM}$, is 0.379 mRy/atom. Both minima are separated by a local maximum at $c/a \approx 1.08$ [28]. The occurrence of the minimum with tetragonal distortion is usual result obtained previously [50].

However, in PM state described by DLM the global minimum in total energy is in cubic austenite and lies 1.756 mRy above the energy of FM austenite. With increasing tetragonal deformation, the total energy increases to 0.070 mRy at $c/a \approx 1.1$ and then it remains almost constant up to $c/a \approx 1.2$. Above that it grows continuously again. There is a shallow local minimum at $(c/a)_{NM} \approx 1.14$, which corresponds to NM phase. Thus, in PM state the NM martensite is destabilized with respect to austenite.

In nonmagnetic (NonM) state, the spin polarization is completely neglected. The energies along the tetragonal deformation path are approximately 20 mRy/atom higher than energies of FM and PM states. A local maximum at c/a = 1, indicates that austenite will be unstable with respect to any tetragonal distortion. A global minimum is located at $(c/a)_{NM}$ = 1.390, which is significantly higher value than for FM state. In addition there is also a local minimum at c/a = 0.875. The absolute value of $\Delta E_{A\text{-}NM}$ = –4.155 mRy/atom is significantly larger compared to other states. This completely different behavior of total energy points out that PM state cannot be approximated by simple neglecting of polarization, but, instead, some description including random orientation of magnetic moments has to be employed. We additionally stress here that total energies along the path for PM state and FM state have been calculated at the same equilibrium volume, which is, however, not the case of NonM state which exhibits about 5% smaller equilibrium volume.

FIG. 2 HERE

Different behavior of total energies in different magnetic states can be understood by analysis of density of states (DOS) displayed in Fig. 2. In NonM state, the austenite exhibits a very high peak at the Fermi level, E_f, which arises from the occupation of Mn-e_g bands with contribution of Ni-e_g antibonding bands. Such high occupation at the E_f explains the high energy of NonM state and its instability. In FM state the occupation at the E_f decreases due to band splitting between majority and minority spin channels, which significantly reduces the total energy. In majority spin channel both e_g bands are pushed to lower energies whereas in minority spin channel the Mn-e_g is unoccupied far above the E_f. However, Ni-e_g band still remains occupied near the E_f, which results in low-temperature instability of FM austenite [51]-[53]. The pseudo gap arising from Ni-Ga covalent interaction [54] can be clearly recognized in FM minority spin channel or in NonM state approximately 0.08 Ry below the E_f. Similar splitting of e_g band as in FM state can be recognized also in PM state. Because Ni atoms carry zero magnetic moments in PM state, which is usual for DLM approach [33], the splitting of e_g band is related only to Mn atoms. The PM state exhibits the same DOS in both spin channels due to overall magnetic moment equal to zero, thus the total occupation near the E_f is slightly higher than in FM state. The pseudo gap is missing in PM state, due to contribution of electrons from both spin channels to DOS. Both described effects result in higher stability of FM state in comparison with PM state.

The NM martensite in FM state is stabilized by Jahn-Teller band effect [51]-[53]. Lowering of symmetry pushes the Ni-e_g antibonding peak above the E_f which decreases the total energy. Similar mechanism can be seen also in NonM state, but here only the Ni-e_g peak is affected by tetragonal distortion whereas the Mn-e_g remains unchanged. The occupation near the E_f is partially lowered which stabilizes the martensitic structure, but the total energy remains still high compare to both magnetic states. The shift of Ni-e_g antibonding peak in PM state due to tetragonal distortion is not so pronounced as in FM and NonM states. The peak is located exactly at the E_f, and consequently the PM state exhibits slightly higher energy in NM martensite than in austenite. However, very small differences between DOS of austenite and NM martensite explain a very flat total energy profile along tetragonal deformation path in PM state.

Further we will discuss the effect of doping on the stability. The effect of Co doping in FM state has been described in our previous work [28] and main results are summarized here in order to compare with new results. Increasing Co concentration with Co replacing Ni ($Ni_{50-x}Co_xMn_{25}Ga_{25}$) destabilizes the NM martensite and decreases the energy barrier between austenite and martensite. In PM state the effect is opposite. Without Co the austenite is stable phase and NM martensite metastable at 0 K (see Fig. 3(a)). Increasing Co concentration stabilizes the NM martensite and slightly increases the barrier between the phases. For 2.5% Co concentration ($Ni_{47.5}Co_{2.5}Mn_{25}Ga_{25}$), the total energy landscape is very flat and varies less than 0.05 mRy/atom in interval $0.975 < c/a < 1.250$, i.e both phases have very similar energies. For 5% Co concentration ($Ni_{45}Co_5Mn_{25}Ga_{25}$) the energy of NM martensite with $(c/a)_{NM} \approx 1.215$ is lower than austenite by about 0.195 mRy/atom. In any case the PM state exhibits energies approximately 2 mRy/atom higher than FM states. Increasing Co concentration in FM state also decreases

the equilibrium $(c/a)_{NM}$ [28]. In contrast, in PM state, the equilibrium $(c/a)_{NM}$ slightly increases with increasing concentration of Co.

FIG. 3 HERE

Stabilization of NM martensite in PM states is even more pronounced for Cu doping (see Fig. 3(b)). The effect is strong for Cu replacing Ga ($Ni_{50}Mn_{25}Ga_{25-z}Cu_z$) and moderate for Cu replacing Mn ($Ni_{50}Mn_{25-y}Ga_{25}Cu_y$). In both cases there is a distinct global minimum on energy profile along tetragonal deformation path at $(c/a)_{NM}$ = 1.265 for Cu replacing Ga and at $(c/a)_{NM}$ = 1.235 for Cu replacing Mn. Contrary to Co doping both PM and FM states exhibit the same qualitative behavior with NM phase stabilized by increasing Cu concentration. As the NM structure has higher energy than austenite in PM state, decreasing of its energy is larger. However, the energy differences $\Delta E_{A\text{-}NM}$ are still smaller than for FM states and thus the martensitic transformation temperature, T_M, could be theoretically lower in PM state.

Related to FM austenite the energies of NM structures are close to each other for both types of doping due to stronger stabilization effect of Cu in Ga sublattice. The main difference between introducing Cu in Ga sites and Cu in Mn sites is in energy difference $\Delta E_{PM\text{-}FM}$, between PM and FM states of austenite (c/a = 1). The doping by 5% Cu instead of Ga ($Ni_{50}Mn_{25}Ga_{20}Cu_5$) exhibits $\Delta E_{PM\text{-}FM}$ = 1.761 mRy/atom, which is almost the same as without doping. In contrast, the same amount of Cu in Mn sites ($Ni_{50}Mn_{20}Ga_{25}Cu_5$) results in smaller $\Delta E_{PM\text{-}FM}$ = 1.097 mRy/atom.

FIG. 4 HERE

The stabilization of NM structure in PM state by doping can also be explained from DOS. The mechanism is roughly the same for all kinds of doping studied in this work, thus only the effect of Co in Ni sites will be explained in detail. The NM structure in PM state exhibits the Ni-e_g antibonding peak exactly at the E_f for stoichiometric composition $Ni_{50}Mn_{25}Ga_{25}$, which destabilizes this structure. Replacing some part of Ni by Co decreases the concentration of valence electrons and changes the position of the E_f with respect to DOS (see Fig. 4). The Ni-e_g peak lies now above the E_f which stabilizes the NM martensite in PM state. Similar shift of Ni-e_g peak above the E_f can found also for Cu doping to Mn or Ga sublattices.

The effects of doping on the energy difference between PM state and FM state, $\Delta E_{PM\text{-}FM}$, are summarized in Fig. 5. From this energy difference we can estimate qualitatively the changes in T_C caused by doping. In austenite, addition of Co destabilizes the PM state and $\Delta E_{PM\text{-}FM}$ increases, which corresponds to experimental finding that T_C^A increases [15]. Effect of Co on T_C^M is not expected to be significant resulting in small decrease in NM martensite, because $\Delta E_{PM\text{-}FM}$ decreases slightly from 2.203 mRy/atom to 2.190 mRy/atom after adding of 5% Co ($Ni_{45}Co_5Mn_{25}Ga_{25}$).

When Cu is added instead of Ga, $\Delta E_{PM\text{-}FM}$ of austenite remains almost constant and thus Curie temperature can be expected to be constant. On the other hand, Cu in Mn sublattice results in steep decrease of $\Delta E_{PM\text{-}FM}$, which can be interpreted as sharp decrease of T_C^A. Both types of Cu doping decrease $\Delta E_{PM\text{-}FM}$ in NM structure, while the effect is much stronger for doping in Mn sublattice than for doping in Ga sublattice. Our prediction agrees with experimental observation, because decreased T_C was observed in alloys which contain Cu [17], [18].

Because simultaneous doping by Co and Cu shows rather independent effects on $\Delta E_{A\text{-}NM}$ and subsequently on T_M [28] or equilibrium lattice parameters, desired properties can be obtained by proper linear combination of dopants. Similar effects can be expected also for $\Delta E_{PM\text{-}FM}$ and subsequently for T_C. Thus the combination Co replacing Ni and Cu replacing Ga should result in increased T_C^A due to major contribution from Co. In addition the same combination should result also in increased T_M and reduced $(c/a)_{NM}$ [29], which was confirmed in experiments on $Ni_{46}Co_4Mn_{24}Ga_{22}Cu_4$ alloy [22], [23].

FIG. 5 HERE

IV. CONCLUSION

The Ni_2MnGa and Co- and Cu- doped Ni_2MnGa alloys have been studied using the EMTO-CPA *ab initio* technique. The ferromagnetic state has been confirmed as a ground state along whole tetragonal deformation path for all studied compositions. Moreover we show that ferromagnetic order is critical for stabilization of NM martensite both stoichiometric Ni_2MnGa as well as in Co and Cu doped material. Although Co doping can increase the T_C of austenite, there is clearly no way to increase the T_C of NM martensite by neither Co nor Cu doping.

ACKNOWLEDGMENT

This research was supported by the Ministry of Education, Youth and Sports of the Czech Republic within the support program “National Sustainability Programme I” (Project NETME CENTRE PLUS – LO1202) [M.Z.] and program OP RDE “Excellent Research Teams” (Project No. CZ.02.1.01/0.0/0.0/15_003/0000487 – MATFUN) [M.Z., L.S., O.H.], by the Czech Science Foundation (Projects No. 16-00043S) [L.S., O.H.] and by the Academy of Finland through the Center of Excellence Program (2012–2017) [R.N.] and Grant No. 277996 [A.S.]. The access to the CERIT-SC computing and storage facilities provided under the program Center CERIT Scientific Cloud, part of the Operational Program Research and Development for Innovations, Reg. No. CZ. 1.05/3.2.00/08.0144 and computational resources from the

Finland IT Center for Science (CSC) and the Aalto Science-IT project is highly acknowledged.

REFERENCES

[1] O. Heczko, N. Scheerbaum, and O. Gutfleisch, "Magnetic Shape Memory Phenomena," in *Nanoscale Magnetic Materials and Applications*, J. P. Liu, E. Fullerton, O. Gutfleisch, and D. J. Sellmyer, Eds. Boston: Springer US, 2009, pp. 399-439.

[2] I. Aaltio, A. Sozinov, Y. Ge, K. Ullakko, V. K. Lindroos, and S.-P. Hannula, "Giant Magnetostrictive Materials," in *Reference Module in Materials Science and Materials Engineering*, S. Hashmi, Ed. Oxford: Elsevier, 2016. pp. 1-14.

[3] S. Wilson *et al*., "New materials for micro-scale sensors and actuators: An engineering review," *Mater. Sci. Eng. R-Rep.*, vol. 56, pp. 1-129, June 2007.

[4] X. Zhou, W. Li, H. P. Kunkel, and G. Williams, "A criterion for enhancing the giant magnetocaloric effect: (Ni–Mn–Ga)—a promising new system for magnetic refrigeration," *J. Phys. Condens. Matter*, vol. 16, pp. L39-L44, Jan. 2004.

[5] P. J. Webster, K. R. A. Ziebeck, S. L. Town, and M. S. Peak, "Magnetic order and phase transformation in Ni_2MnGa," *Philos. Mag. B*, vol. 49, pp. 295-310, 1984.

[6] S. J. Murray, M. A. Marioni, S. M. Allen, R. C. O'Handley, and T. A. Lograsso, "6% magnetic-field-induced strain by twin-boundary motion in ferromagnetic Ni–Mn–Ga," *Appl. Phys. Lett.*, vol. 77, pp. 886-888, Aug. 2000.

[7] O. Heczko, A. Sozinov, and K. Ullakko, "Giant field-induced reversible strain in magnetic shape memory NiMnGa alloy," *IEEE Trans. Magn.*, vol. 36, pp. 3266-3288, Aug. 2000.

[8] M. Zelený, L. Straka, A. Sozinov, and O. Heczko, "*Ab initio* prediction of stable nanotwin double layers and 4O structure in Ni_2MnGa," *Phys. Rev. B*, vol. 94, p. 224108, Dec. 2016.

[9] A. Sozinov, A. A. Likhachev, N. Lanska, and K. Ullakko, "Giant magnetic-field-induced strain in NiMnGa seven-layered martensitic phase," *Appl. Phys. Lett.*, vol. 80, pp. 1746-1748, Mar. 2002.

[10] A. Çakır, L. Righi, F. Albertini, M. Acet, M. Farle, and S. Aktürk, "Extended investigation of intermartensitic transitions in Ni-Mn-Ga magnetic shape memory alloys: A detailed phase diagram determination," *J. Appl. Phys.*, vol. 114, p. 183912, Nov. 2013.

[11] C. Jiang, Y. Muhammad, L. Deng, W. Wu and H. Xu, "Composition dependence on the martensitic structures of the Mn-rich NiMnGa alloys," *Acta Matter.*, vol. 52, pp. 2779-2785, Mar. 2004.

[12] A. N. Vasil'ev *et al.*, "Structural and magnetic phase transitions in shape-memory alloys $Ni_{2+x}Mn_{1-x}Ga$," *Phys. Rev. B*, vol. 59, pp. 1113-1120, Jan. 1999.

[13] P. Entel *et al.*, "Modelling the phase diagram of magnetic shape memory Heusler alloys," *J. Phys. D: Appl. Phys.*, vol. 39 pp. 865–889, Feb. 2006.

[14] I. Galanakis and E. Şaşıoğlu, "Variation of the magnetic properties of Ni_2MnGa Heusler alloy upon tetragonalization: a first-principles study," *J. Phys. D: Appl. Phys.*, vol. 44, p. 235001, May 2011.

[15] D. E. Soto-Parra *et al.*, "Fe and Co selective substitution in Ni_2MnGa: Effect of magnetism on relative phase stability," *Philos. Mag.*, vol. 90, pp. 2771-2792, July 2010.

[16] V. Sokolovskiy, A. Grünebohm, V. Buchelnikov, and P. Entel, "*Ab initio* and Monte Carlo approaches for the magnetocaloric effect in Co- and In-doped Ni-Mn-Ga Heusler alloys," *Entropy*, vol. 16, pp. 4992-5019, Sept. 2014.

[17] I. Glavatskyy, N. Glavatska, A. Dobrinsky, J.-U. Hoffmann, O. Söderberg, and S.-P. Hannula, "Crystal structure and high-temperature magnetoplasticity in the new Ni–Mn–Ga–Cu magnetic shape memory alloys," *Scripta Mater.*, vol. 56 pp. 565-568, Apr. 2007.

[18] C. B. Jiang, J. M. Wang, P. P. Li, A. Jia, and H. B. Xu, "Search for transformation from paramagnetic martensite to ferromagnetic austenite: NiMnGaCu alloys," *Appl. Phys. Lett.*, vol. 95, p. 012501, July 2009.

[19] A. T. Zayak, P. Entel, K. M. Rabe, W. A. Adeagbo, and M. Acet, "Anomalous vibrational effects in nonmagnetic and magnetic Heusler alloys," *Phys. Rev. B*, vol. 72, p. 054113, Aug. 2005.

[20] S. Roy *et al.*, "Delocalization and hybridization enhance the magnetocaloric effect in Cu-doped Ni_2MnGa," *Phys. Rev. B*, vol. 79, p. 235127 June 2009.

[21] G. J. Li *et al.*, "Role of covalent hybridization in the martensitic structure and magnetic properties of shape-memory alloys: The case of $Ni_{50}Mn_{5+x}Ga_{35-x}Cu_{10}$," *Appl. Phys. Lett.*, vol. 102, p. 062407, Feb. 2013.

[22] A. Sozinov, N. Lanska, A. Soroka, and W. Zou, "12% magnetic field-induced strain in Ni-Mn-Ga-based non-modulated martensite," *Appl. Phys. Lett.*, vol. 102, p. 021902, Jan. 2013.

[23] A. Sozinov, A. Soroka, N. Lanska, M. Rameš, L. Straka, and K. Ullakko, "Temperature dependence of twinning and magnetic stresses in $Ni_{46}Mn_{24}Ga_{22}Co_4Cu_4$ alloy with giant 12% magnetic field-induced strain," *Scripta Mater.*, vol. 131, pp. 33-36, Jan. 2017.

[24] P. Hohenberg and W. Kohn, "Inhomogeneous electron gas," *Phys. Rev.*, vol. 136, pp. B864-B871, Nov. 1964.

[25] W. Kohn and L. J. Sham, "Self-consistent equations including exchange and correlation effects," *Phys. Rev.*, vol. 140, pp. A1133-A1138, Nov. 1965.

[26] C.-M. Li, H. B. Luo, Q.-M. Hu, R. Yang, B. Johansson, and L. Vitos, "Site preference and elastic properties of Fe-, Co-, and Cu-doped Ni_2MnGa shape memory alloys from first principles," *Phys. Rev.* B, vol. 84, p. 024206, July 2011.

[27] J. Chen, Y. Li, J. X. Shang, and H. B. Xu, "First principles calculations on martensitic transformation and phase instability of Ni–Mn–Ga high temperature shape memory alloys," *Appl. Phys. Lett.*, vol. 89, p. 231921, Dec. 2006.

[28] M. Zelený, A. Sozinov, L. Straka, T. Björkman, and R. M. Nieminen, "First-principles study of Co- and Cu-doped Ni_2MnGa along the tetragonal deformation path," *Phys. Rev. B*, vol. 89, p. 184103, May 2014.

[29] M. Zelený, A. Sozinov, L. Straka, T. Björkman, and R. M. Nieminen, "*Ab initio* study of properties of Co- and Cu- doped Ni-Mn-Ga alloys," *Mater. Today: Proceedings*, vol. 2S, pp. S601-S604, Nov. 2015.

[30] P. Entel *et al.*, "Fundamental aspects of magnetic shape memory alloys: Insights from *ab initio* and Monte Carlo studies," *Mater. Sci. Forum*, vol. 635, pp. 3-12. Dec. 2009.

[31] P. Entel *et al.*, "Basic properties of magnetic shape-memory materials from first-principles calculations," *Metall. and Mat. Trans. A*, vol. 43, pp. 2891-2900, Aug. 2012.

[32] V. V. Sokolovskiy, O. Pavlukhina, V. D. Buchelnikov, and P. Entel, "Monte Carlo and first-principles approaches for single crystal and polycrystalline Ni_2MnGa Heusler alloys," *J. Phys. D: Appl. Phys.*, vol. 47, p. 425002, Sept. 2014.

[33] I. Turek, "*Ab initio* calculations of Curie temperatures," in *Encyclopedia of Materials: Science and Technology*, 2nd ed., K.H. J. Buschow *et al.* Eds. Oxford: Elsevier, 2008, pp. 1-6.

[34] J. B. Staunton, "The electronic structure of magnetic transition metallic materials," *Rep. Prog. Phys.*, vol. 57, pp. 1289-1344, Dec. 1994.

[35] B. Dutta, S. Bhandary, S. Ghosh, and B. Sanyal, "First-principles study of magnetism in Pd_3Fe under pressure," *Phys. Rev. B*, vol. 86, p. 024419, July 2012.

[36] B. L. Gyorffy, J. A. Pindor, J. Staunton, G. M. Stocks, and H. Winter, "A first-principles theory of ferromagnetic phase transitions in metals," *J. Phys. F: Met. Phys.*, vol. 15, pp. 1337–1386, June 1985.

[37] L. Vitos, *Computational Quantum Mechanics for Materials Engineers*, London: Springer, 2007.

[38] O. K. Andersen, O. Jepsen, and G. Krier, "Exact Muffin-Tin Orbital Theory," in *Lectures on Methods of Electronic Structure Calculations*, V. Kumar, O. K. Andersen, and A. Mookerjee, Eds. Singapore: World Scientific Publishing Co., 1994, pp. 63-124.

[39] L. Vitos, H. Skriver, B. Johansson, and J. Kollár, "Application of the Exact Muffin-tin Orbitals Theory: the Spherical Cell Approximation," *Comp. Mat. Sci.* vol. 18, pp. 24-38, July 2000.

[40] L. Vitos, J. Kollár, and H. L. Skriver, "Full charge-density scheme with a kinetic-energy correction: Application to ground-state properties of the 4d metals," *Phys. Rev. B*, vol. 55, p. 13521-13527, May 1997.

[41] P. Soven, "Coherent-Potential Model of Substitutional Disordered Alloys," *Phys. Rev.*, vol. 156, 809-813, Apr. 1967.

[42] L. Vitos, I. A. Abrikosov, and B. Johansson, "Anisotropic Lattice Distortions in Random Alloys from First-Principles Theory," *Phys. Rev. Lett.*, vol. 87, p. 156401, Sept. 2001.

[43] K. Özdoğan, E. Şaşıoğlu, and I. Galanakis, "Engineering the electronic, magnetic, and gap-related properties of the quinternary half-metallic Heusler alloys," *J. Appl. Phys.*, vol. 103, p. 023503, Jan. 2008.

[44] M. Zelený and I. Dlouhý, "Different *ab initio* approaches for doping descriptions: Tetragonal deformation of Ni-Mn-Ga alloys," *Solid State Phenom.*, vol. 258, pp. 37-40, 2017.

[45] J. P. Perdew, K. Burke, and M. Ernzerhof, "Generalized gradient approximation made simple," *Phys. Rev. Lett.*, vol. 77, pp. 3865-3868, Oct. 1996.

[46] Q.-M. Hu, H.-B. Luo, C.-M. Li, L. Vitos, and R. Yang, "Composition dependent elastic modulus and phase stability of Ni_2MnGa based ferromagnetic shape memory alloys", *Sci. China Tech. Sci.*, vol. 55, pp. 295-305, Feb. 2012.
[47] C.-M. Li, Q.-M. Hu, R. Yang, B. Johansson, and L. Vitos, "Interplay between temperature and composition effects on the martensitic transformation in $Ni_{2+x}Mn_{1-x}Ga$ alloys," *Appl. Phys. Lett.*, vol. 98, pp. 261903, June 2011.
[48] P. A. Korzhavyi, A. V. Ruban, I. A. Abrikosov, and H. L. Skriver, "Madelung energy for random metallic alloys in the coherent potential approximation", *Phys. Rev. B*, vol. 51, pp. 5773, March 1995.
[49] A. V. Ruban and H. L. Skriver, "Screened Coulomb interactions in metallic alloys. I. Universal screening in the atomic-sphere approximation", *Phys. Rev. B*, vol. 66, pp. 024201, June 2002.
[50] A. Ayuela, J Enkovaara, K. Ullakko, and R. M. Nieminen, "Structural properties of magnetic Heusler alloys," *J. Phys.: Condens. Matter*, vol. 11, pp. 2017-2026, Mar. 1999.
[51] S. Fujii, S. Ishida, and S. Asano, "Electronic structure and lattice transformation in Ni_2MnGa and Co_2NbSn," *J. Phys. Soc. Jpn.*, vol. 58, pp. 3657-3665, Oct. 1989.
[52] P. J. Brown, A. Y. Bargawi, J. Crangle, K. U. Neuman, and K. R. A. Ziebeck, "Direct observation of a band Jahn-Teller effect in the martensitic phase transition of Ni_2MnGa," *J. Phys. Condens. Matter*, vol. 11, pp. 4715-4722, June 1999.
[53] S. Ö. Kart, M. Uludoğan, I. Karaman, and T. Çağın, "DFT studies on structure, mechanics and phase behavior of magnetic shape memory alloys: Ni_2MnGa," *Phys. Stat. Sol. (a)*, vol. 205, pp. 1026-1033, Mar. 2008.
[54] C.-M. Li, H.-B. Luo, Q.-M. Hu, R. Yang, B. Johansson, and L. Vitos, "First-principles investigation of the composition dependent properties of $Ni_{2+x}Mn_{1-x}Ga$ shape-memory alloys," *Phys. Rev. B.*, vol. 82, p. 024201, July 2010.

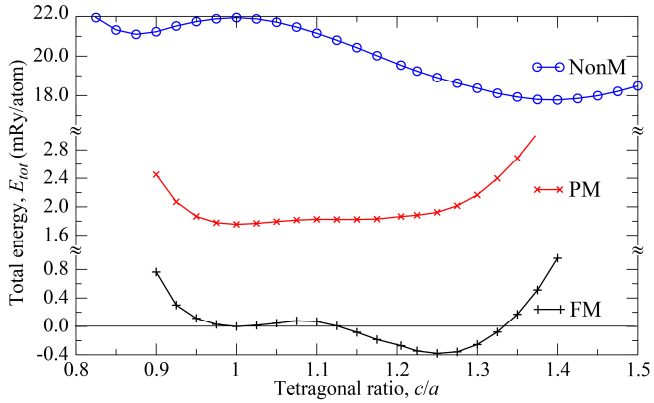

Fig. 1. Total energy as a function of tetragonal ratio c/a for alloys with stoichiometric composition Ni_2MnGa in ferromagnetic (FM – black solid line), paramagnetic (PM – red solid line) and nonmagnetic (NonM – blue solid line) states. All energies are related to the energy of the cubic structure in FM state.

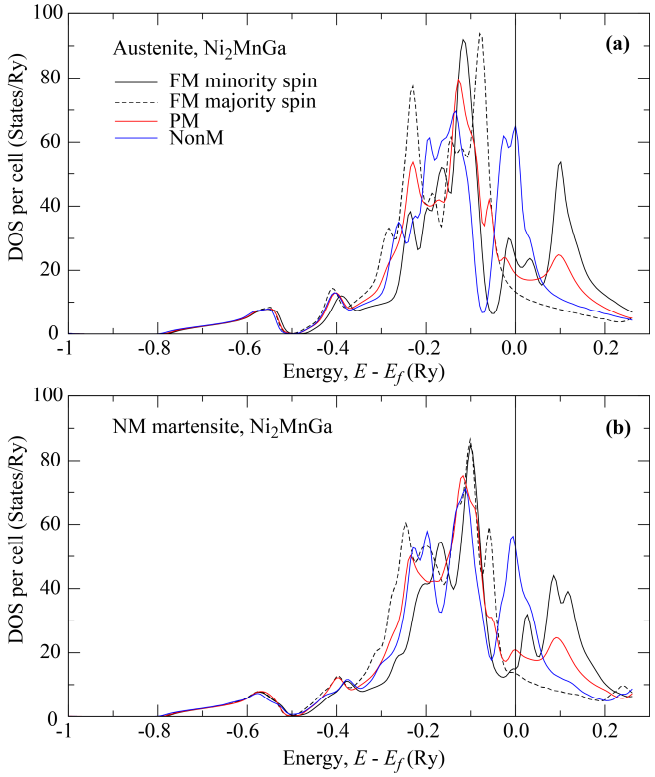

Fig. 2. The density of state (DOS) of alloys with stoichiometric composition Ni_2MnGa in austenite (a) and NM martensite (b). For ferromagnetic (FM) state the DOS are shown separately for minority spin channel (black solid line) and majority spin channel (black dashed line) whereas for paramagnetic (PM – red solid line) and nonmagnetic (NonM – blue solid line) states are DOS the same in both spin channel. The zero energy corresponds to the Fermi level, E_f.

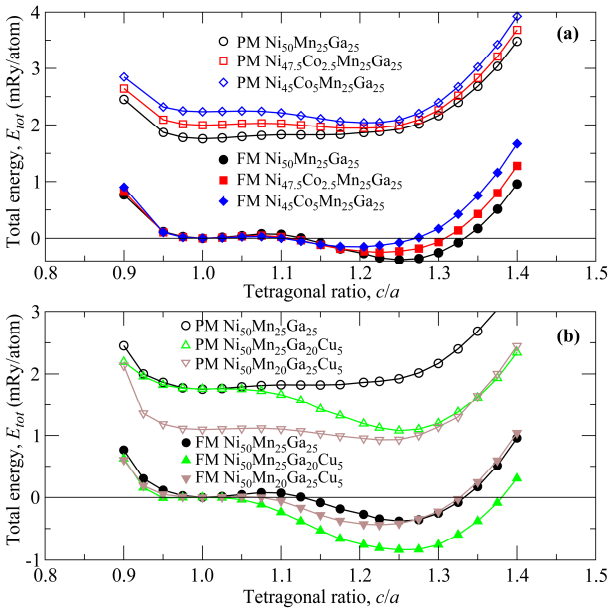

Fig. 3. Total energy as a function of tetragonal ratio c/a for Co-doped alloys with composition $Ni_{50-x}Co_xMn_{25}Ga_{25}$ (a) and Cu-doped alloys (b) with compositions $Ni_{50}Mn_{25}Ga_{20}Cu_5$ and $Ni_{50}Mn_{20}Ga_{25}Cu_5$ in ferromagnetic (FM – full symbols) and paramagnetic (PM – open symbols) states. All energies are related to the energy of the cubic structure in FM state of alloy with given composition.

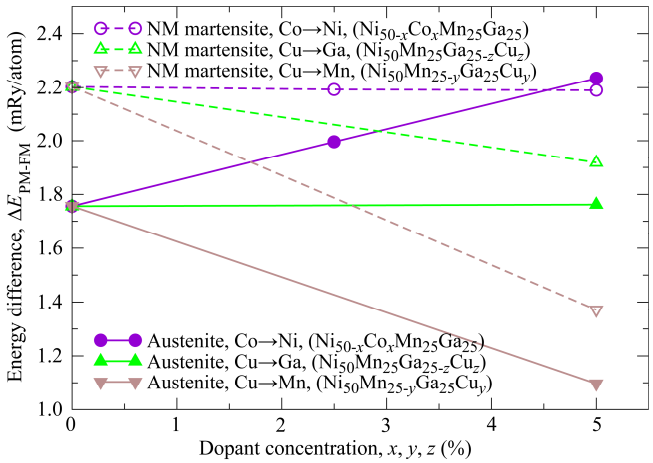

Fig. 5. Total energy differences between the paramagnetic (PM) and ferromagnetic (FM) states, ΔE_{PM-FM}, in austenite and NM martensite as a function of dopant concentration x, y or z for different alloys with general compositions $Ni_{50-x}Co_xMn_{25-y}Ga_{25-z}Cu_{y+z}$.

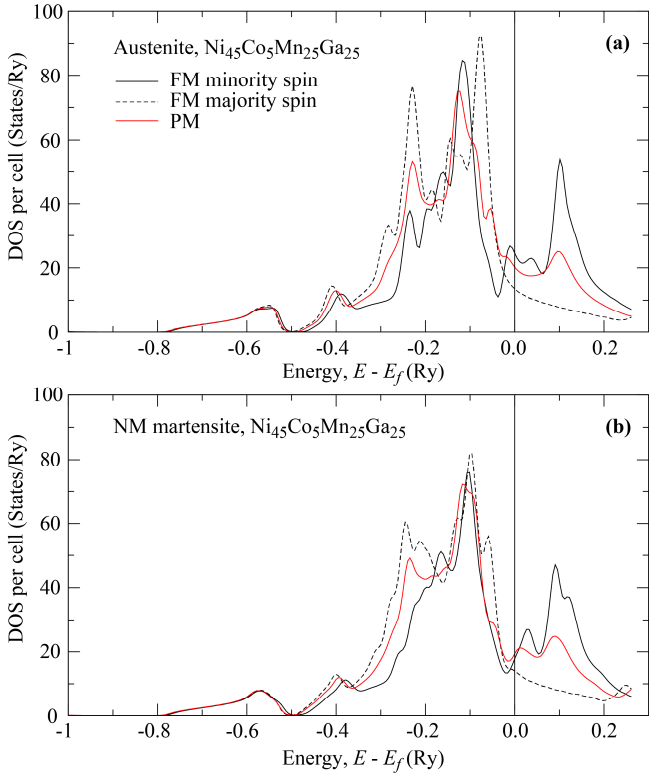

Fig. 4. The density of state (DOS) of alloys with composition $Ni_{45}Co_5Mn_{25}Ga_{25}$ in austenite (a) and NM martensite (a). For ferromagnetic (FM) state the DOS are shown separately for minority spin channel (black solid line) and majority spin channel (black dashed line) whereas for paramagnetic (PM – red solid line) state is DOS the same in both spin channel. The zero energy corresponds to the Fermi level, E_f.